PHYSICAL REVIEW B, VOLUME 64, 045211

Electronic structure of thiophenes and phtalocyanines

E. Z. Kurmaev, S. N. Shamin, and V. R. Galakhov
Institute of Metal Physics, Russian Academy of Sciences-Ural Division, 620219 Yekaterinburg GSP-170, Russia

A. Moewes
University of Saskatchewan, Department of Physics and Engineering Physics, 116 Science Place, Saskatoon, SK S7N 5E2, Canada

T. Otsuka, S. Koizume, and K. Endo
Department of Chemistry, Faculty of Science, Kanazawa University, Kakuma-machi, Kanazawa, 920-1192 Japan

H. E. Katz
Bell Laboratories, Lucent Technologies, Murray Hill, New Jersey 07974

M. Bach and M. Neumann
Universität Osnabrück, Fachbereich Physik, D-49069 Osnabrück, Germany

D. L. Ederer
Department of Physics, Tulane University, New Orleans, Louisiana 70118

M. Iwami
Research Laboratory for Surface Science, Okayama University, Okayma 700-8530, Japan

(Received 20 December 2000; published 6 July 2001)

The results of x-ray fluorescence measurements of thiophenes [regioregular poly (3-hexylthiophene (P3HT) and α,ω-dihexylquaterthiophene (DHα4T)] and phtalocyanines [copper phtalocyanine (CuPc) and copper hexadecafluorophtalocyanine (F_{16}CuPc)] are presented. Experimental carbon, nitrogen, fluorine $K\alpha$ and sulphur, copper $L_{2,3}$ x-ray emission spectra are compared with ultraviolet photoemission spectroscopy spectra and deMon density-functional theory calculations of model molecules. We find that the carbon $K\alpha$ emission is almost identical for P3HT and DHα4T. This indicates that the electronic structure of the π system is not affected by the presence of the side group. The ratio of emission intensities of the Cu L_2 to Cu L_3 intensities is found to be smaller by a factor of 2 for CuPc and F_{16}CuPc than it is for pure metal. This demonstrates the strong covalency in phalocyanines.

DOI: 10.1103/PhysRevB.64.045211 PACS number(s): 78.70.En, 71.20.Rv, 72.80.Le

I. INTRODUCTION

Organic materials are of potential use as semiconducting layer in field-effect transistors (FET's) because they are easily processed and compatible with plastic substrates.[1–3] Since the first report in 1987,[4] the performance of organic FET's has continuously improved and now they can compete with other conventional thin-film transistors (TFT's) such as amorphous silicon devices. For instance, on-off ratios of organic FET's are in the 10^9 range, whereas those of a-Si:HTFT's are limited to 10^6.[3]

Thin-film transistors with active materials of oligomers of thiophene are p-channel transistors and work in the accumulation and depletion mode. It is shown that field-effect mobilities of $\mu = 0.01$ to $0.05\ \mathrm{cm}^2\,\mathrm{V}^{-1}\,\mathrm{s}^{-1}$ and on-off current ratios greater than 10^6 are achievable with such materials.[5]

Up to now, most of the organic and polymeric semiconductors, used as FET's are p-channel materials and only few compounds are found to function as n-channel semiconductors. Among them, C_{60} and C_{70} are reported[6–7] to have the highest field-effect mobility (about to $0.08\ \mathrm{cm}^2\,\mathrm{V}^{-1}\,\mathrm{s}^{-1}$). However, those devices are highly air sensitive, which poses difficulties in terms of practical applications. Recently, hexadecahalogenated metallophtalocyanines were found to function as air-stable n-channel semiconductors with maximum electron-field effect mobility of $0.03\ \mathrm{cm}^2\,\mathrm{V}^{-1}\,\mathrm{s}^{-1}$.[8]

It is found that n-channel organic semiconductors operate in the accumulation mode and, like the oligothiophenes, can never operate in the inversion mode. Therefore, it is not possible to realize n and p-channel operation in a single material. An organic transistor structure has been developed with two active materials that permit both p-channel and n-channel operation in a single device.[5] The two active materials are chosen for the following two reasons: Their previous performance as p-channel and n-channel transistors and the favorable energy levels of their highest occupied and lowest unoccupied molecular orbitals. Conclusively a study of the electronic orbital structure of potential candidates for organic heterostructures FET's is important.

In the present paper we report the results of first x-ray fluorescence measurements of thiophenes [regioregular poly 3-hexylthiophene (P3HT) and α,ω-dihexylquaterthiophene (DHα4T)] and phtalocyanines [copper phtalocyanine (CuPc) and copper hexadecafluorophtalocyanine (F_{16}CuPc)]. We have measured soft x-ray emission spectra (XES) of these compounds. The obtained results are compared with ultraviolet photoemission spectra (UPS) and deMon density-functional theory[9] (DFT) calculations of model molecules.

II. EXPERIMENTAL AND CALCULATION DETAILS

The carbon, nitrogen, and fluorine $K\alpha$ ($2p \rightarrow 1s$ transition), sulphur $L_{2,3}$ ($3d3s \rightarrow 2p_{3/2,1/2}$ transition) and Cu $L_{2,3}$ ($3d4s \rightarrow 2p_{3/2,1/2}$ transition) XES were recorded at the Advanced Light Source (Beamline 8.0) at Lawrence Berkeley National Laboratory, employing the soft x-ray fluorescence endstation.[10] Photons with an energy above the carbon K edge (310 eV), with an energy above the nitrogen K edge (430 eV), with an energy above the fluorine K edge (720 eV), with an energy above the sulphur L edge (180 eV), and with an energy above the copper L edge (970 eV) were delivered to the endstation via the beamline's undulator and spherical grating monochromator. The carbon and nitrogen $K\alpha$ spectra were obtained with a 600 lines/mm, 10-m radius grating and energy resolution of 0.3–0.4 eV. The sulphur $L_{2,3}$ emission spectra were measured with a 1500 lines/mm, 5-m radius grating and energy resolution of 0.4 eV. Fluorine $K\alpha$ x-ray emission spectra were recorded using a fluorescence spectrometer with a 1500 lines/mm 10 m radius grating and energy resolution of 0.9 eV. Copper $L_{2,3}$ XES were measured with $N = 600$ lines/mm, $R = 10$-m diffraction grating and energy resolution of 1.2 eV.

The X-ray photoemission spectroscopy (XPS) measurements of core levels have been carried out with a PHI5600 ci-type ESCA spectrometer using monochromatized Al $K\alpha$ radiation with 0.3 eV full width and half maximum (FWHM). The energy resolution of the analyzer was 1.5% of the pass energy. We estimate the energy resolution of the spectrometer to be better than 0.35 eV. The pressure in the vacuum chamber during the measurements was below 5×10^{-9} mbar. All measurements were performed at room temperature. The XPS spectra were calibrated using the Au $4f_{7/2}$ signal from Au foil, which has a binding energy of 84.0 eV.

The thiophenes [regioregular poly(3-hexylthiophene (P3HT)] and phtalocyanines [copper phtalocyanine (CuPc) and copper hexadecafluorophtalocyanine (F_{16}CuPc)] were purchased and α,ω-dihexylquaterthiophene (DHα4T) was synthesized under conditions described in Ref. 11.

DeMon DFT calculations[9] of organic semiconductors were performed using model molecules. For model molecules, we used a monomer molecule $\{\mathrm{Cu\text{-}C_{32}N_8H_{16}}\}$ for CuPc, three thiophene rings $\{\mathrm{C_4SH_2(C_6H_{13})}\} - \{\mathrm{C_4SH_2(C_6H_{13})}\} - \{\mathrm{C_4SH_2(C_6H_{13})}\}$ for P3HT and the model molecule $\{\mathrm{H\text{-}(C_4H_2S)_3\text{-}H}\}$ for DHα4T, respectively.

Our calculations of XES spectra are based on an experimental description of the electronic structure of the compound. The energy position of the spectral lines correspond to the differences between the total energies of the various excited final-state wave functions Φ_f, and the initial-state wave functions Φ_i. The intensity of the line is given by

$$\tau_{if} \propto \left| \int \Phi_i P \Phi_f d_\tau \right|^2, \qquad (1)$$

where P is the associated transition operator. For x-ray emission spectra, the transitions are governed by dipole selection rule and the orbital angular momentum quantum number is constrained to change according to the relation $\Delta l = \pm 1$. For example, the observed electron transitions in the atoms (of light elements) arise from the filling of s-type ($l = 0$) holes by occupied orbitals with p character ($l = 1$) in the same atom. We can obtain the calculated values for the XES emission energies from the differences between the core-level binding energies (CEBE) and the vertical ionization potentials (VIP's) of the electrons that refill the core hole.

For the geometry of the molecules, we used the optimized Cartesian coordinate from the semiempirical AM1 (version 6.0) method.[12] DeMon calculations were performed with the exchange-correlation potential labeled as B88/P86, made from Becke's 1988 exchange functional[13] and Perdew's 1986 correlation functional.[14] In the program, we used a nonrandom grid and polarized valence double-ς basis of (621/41/1*) for C and N, (41) for H, (6321/521/1*) for S, and (63321/531*/41+) for Cu with auxiliary fitting functions labeled (4, 4; 4, 4) for C and N, (3, 1; 3, 1) for H, (5, 4; 5, 4) for S, and (5, 5; 5, 5) for Cu. In order to calculate each intensity of valence XPS and XES for model molecules, we considered only the atoms of the model molecule. We also used the STO-3G basis set for each atom of the model molecules to calculate the intensity of the emission spectra.

Each peak in the theoretical XES spectra is also represented by a Gaussian line-shape function, with the same weight and FWHM $= 0.65$ eV as the experimental spectra.

A more consistent treatment of the excitations can be done in a quasiparticle band-structure calculation, using a GW approximation (see Ref. 29). On the basis of calculations performed for various materials, the quasiparticle band structure in most cases (when correlation effects are not particularly strong) is well represented by Kohn-Sham one-particle energies, at least the occupied Kohn-Sham states. A discussion on this subject [that relates the local-density approximation (LDA)+U method, developed as a special nonlocal extension to LDA for the treatment of correlated systems, to a certain approximation within the GW approach] can be found in a review by Anisimov, Aryasetiawan and Lichtenstein.[30] If correlations (beyond LDA) can be neglected, the LDA itself can be considered as an approximation to the quasiband band structure.

III. RESULTS AND DISCUSSION

Nonresonant x-ray emission spectra are measured by exciting above the core ionization threshold. The intensity distribution of nonresonant soft x-ray emission spectra of light elements maps the p density at each particular atomic site, and in a molecular orbital picture, the contribution of the local p-type atomic orbitals.

A. Phtalocyanines

Figure 1 shows C $K\alpha$, N $K\alpha$, and Cu$L_{2,3}$ XES of CuPc and F_{16}CuPc. The spectra of reference samples [benzene,[15] pyridine,[16] copper, CuO and Cu_2O (Ref. 17)] are displayed

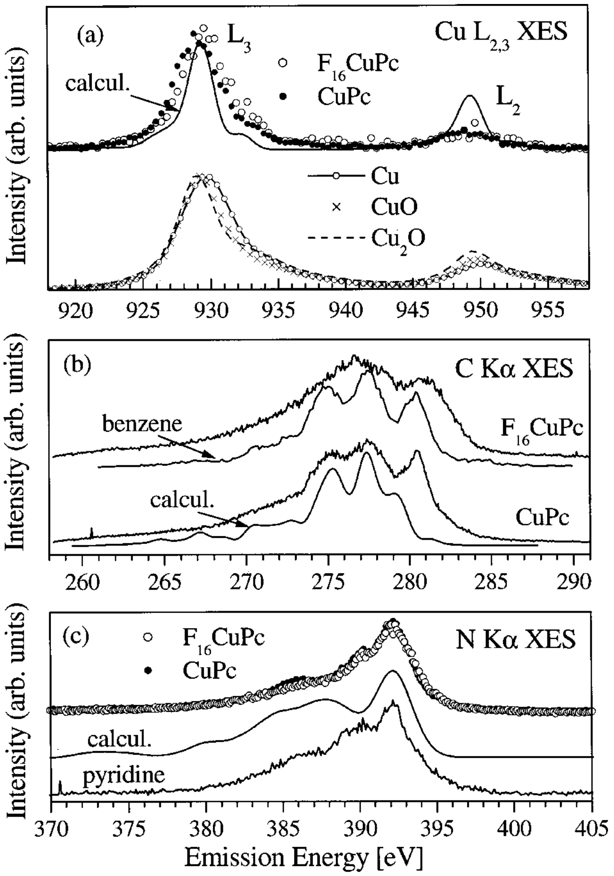

FIG. 1. Experimental and calculated Cu $L_{2,3}$, C $K\alpha$, and N $K\alpha$ XES of phtalocyanines.

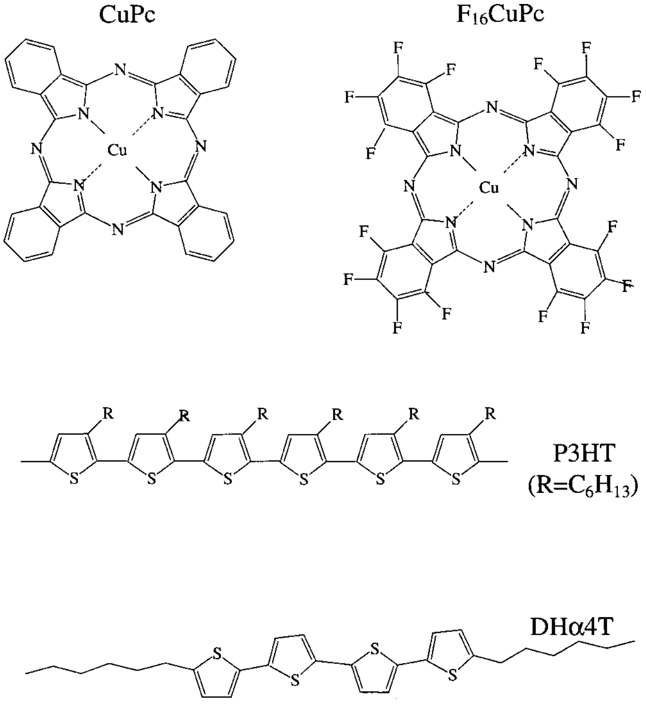

FIG. 2. Chemical structures of phtalocyanines and thiophenes.

for comparison. The x-ray transitions are localized within the first coordination sphere of particular atoms, which results in high sensitivity of XES to the local surrounding of the emitting atoms. Copper atoms have the same surrounding in CuPc and F_{16}CuPc as shown in Fig. 2, and as a result the Cu$L_{2,3}$ emission spectra, which probe Cu $3d4s$ densities of occupied states, are practically identical in both compounds [Fig. 1(a)]. The intensity ratio of L_2 to L_3 lines in CuPc and F_{16}CuPc is rather small (0.16) and smaller than in pure Cu metal (0.22) or copper monoxide (0.32) where copper has the same oxidation state (Cu^{2+}). The ratio of intensities of L_2 ($3d4s \rightarrow p_{1/2}$ transition) emission to L_3 ($3d4s \rightarrow 2p_{3/2}$ transition) the emission differs from the value of 1/2 as one would expect from the occupancy of L_2 and L_3 levels. It strongly depends on the chemical state of the elements.[18] For the spectra of $3d$ metals, the ratio L_2 to L_3 is very small due to radiationless Coster-Kronig process $L_2L_3M_{4,5}$.[19] The probability of $L_2L_3M_{4,5}$ Coster-Kronig transitions is distinctly lower for $3d$ oxides than for metals due to the presence of an energy gap. The $I(L_2)/I(L_3)$ intensity ratio should increase from pure metals to metal oxides.[20] However, the L_2/L_3 ratio decreases in the sequence MnO-Mn_2O_3-MnO_2 (Ref. 21) due to increasing covalency. The low ratio of L_2/L_3 for CuPc and F_{16}CuPc is likely to be due to strong covalency in phtalocyanines. This interpretation is in a good agreement with measurements of fluorine $K\alpha$ XES of F_{16}CuPc as displayed in Fig. 3. It shows a high-energy chemical shift of 0.8 eV with respect to CuF_2, another Cu^{2+} ionic compound. Our conclusion is also supported by previous $2p_{3/2,1/2}$ photoemission experiments of CuPc and CuO.[22] According to this paper, the intensity of the shake-up satellite relative to the main line—which is a measure of the covalency in cupric compounds—is less for CuPc than for CuO.

Nitrogen $K\alpha$ XES is found to be identical for CuPc and F_{16}CuPc, which is not unexpected because emitting atoms, in this case, have the same local surrounding in both compounds. On the other hand, these spectra resemble N $K\alpha$ XES of pyridine (C_6H_5N)[16] [see Fig. 1(c)] in spite of some differences in the chemical structure.

Figure 1(b) shows that the fine structure of C $K\alpha$ emission is very different for CuPc and F_{16}CuPc. The spectral features for F_{16}CuPc are broader than for CuPc but both compounds disclose the same three-peak structure typical for phenyl rings as showcased by the spectrum of benzene in Fig. 1(b). The broadening can be attributed to additional C-F

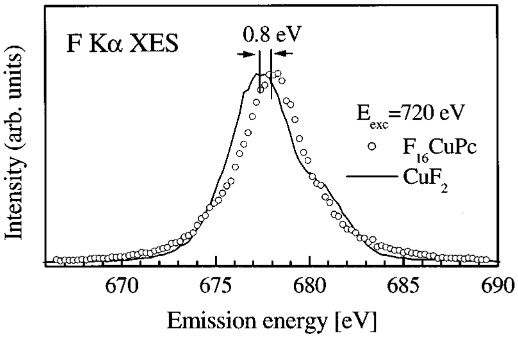

FIG. 3. F $K\alpha$ XES of F_{16}CuPc and CuF_2.

TABLE I. Observed peaks, emission energy, orbital nature, and functional group for C $K\alpha$ XES of CuPc.

Observed peaks (eV)	Emission energy[a] [CEBE-VIP] (eV)	Orbital nature	Functional group
272	263.0–271.8	s_σ(N2s-C2sC2p)-B	-N═C
(260–274)[b]	272.3–275.3	p_σ(C2s-C2p)-B	-C═C
275	275.8–278.0	p_π(C2p-N2p)-B	-N═C
(274–276)[b]			
278	278.0–280.9	p_π(C2p-N2p)-B	-N═C
(276–279)[b]			
280.5	281.0–284.8	p_π(C2p-C2p)-B	-C═C
(279–283)[b]			

[a] Emission energy $[(\mathrm{CEBE})_{ls}-(\mathrm{VIP},I_k)]_{j[2p(A)]}$ is obtained from the difference between core-level binding energies(CEBE) and the vertical ionization potentials (VIP's) of the electrons that refill the core hole.

[b] Peak range.

interactions due to the appearance of fluorine side groups in the chemical structure of F$_{16}$CuPc (Fig. 2).

The calculated Cu $L_{2,3}$, C $K\alpha$, and N $K\alpha$ XES of CuPc (see Fig. 1 and Tables I and II) are in good agreement with the experimental data. Details for the calculations are summarized in the tables. DeMon DFT calculations show that the main features of C $K\alpha$ XES of CuPc are formed by p_π(C2p-C2p) bonding orbitals of -C═C and -N═C functional groups. The main maximum of N $K\alpha$ XES of CuPc is formed by d_π-p_π(Cu3d-N2p),p_π(Cu4p-N2p), p_σ(Cu4s-N2p) bonding orbitals of -Cu═N functional groups and p_π(C2p-N2p) bonding orbitals of -N═C functional groups.

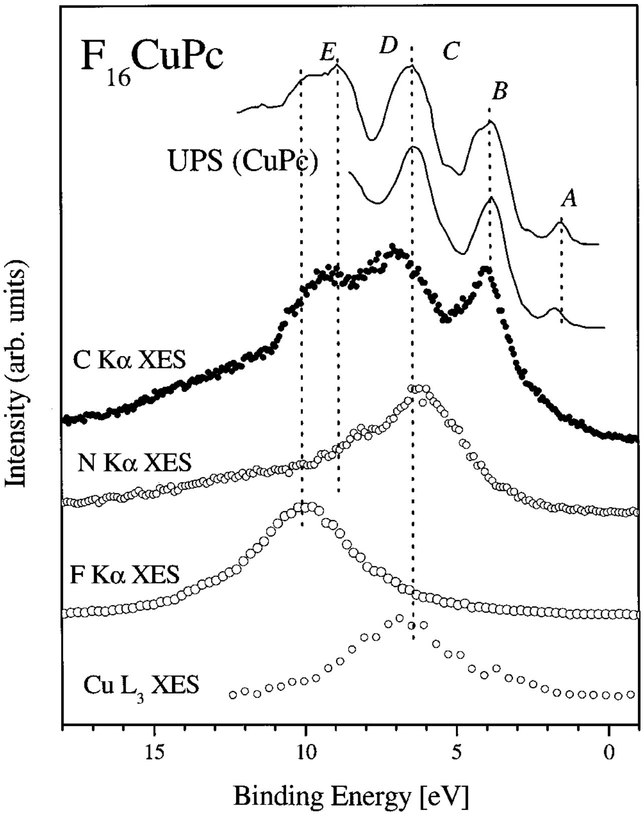

FIG. 4. Comparison of x-ray emission spectra of constituents of F$_{16}$CuPc in the binding-energy scale. UPS of CuPc is taken from Refs. 23 and 24.

Figure 4 shows the comparison between x-ray emission spectra of constituents and UPS of F$_{16}$CuPc. UPS of CuPc (taken from Refs. 23 and 24) is shown in the figure for comparison. All spectra have been converted to the binding energy scale using our XPS measurements of binding energies of the core levels. Element and symmetry selectivity in x-ray emission is helpful in the assignment of the main peaks of UPS spectra. In the region 14–8 eV the contributions of

TABLE II. Observed peaks, emission energy, orbital nature, and functional group for N $K\alpha$ XES of CuPc.

Observed peaks (eV)	Emission energy[a] [CEBE-VIP] (eV)	Orbital nature	Functional group
385	376.2–384.2	s_σ(N2sN2p-C2s)-B	-N═C
(370–388)[b]	386.0–390.9	p_σ(C2s-N2p)-B	-N═C
390	391.0–394.1	p_π(C2p-N2p)-B	-N═C
(388–391)[b]		d_π-p_π(Cu3d-N2p)-B	-Cu-N═
393	394.3–398.6	d_π-p_π(Cu3d-N2p)-B	-Cu-N═
(391–396)[b]		p_π(Cu4p-N2p)-B	-Cu-N═
		p_σ(C4s-N2p)-B	-Cu-N═
		p_π(C2p-N2p)-B	-N═C

[a] The emission energy $[(\mathrm{CEBE})_{ls}-(\mathrm{VIP},I_k)]_{j[2p(A)]}$ is obtained from the difference between core-level binding energies(CEBE) and the vertical ionization potentials (VIP's) of the electrons that refill the core hole.

[b] Peak range.

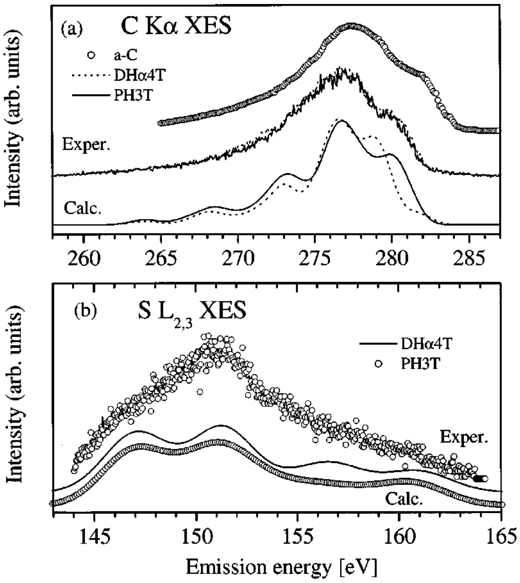

FIG. 5. Experimental and calculated C $K\alpha$ and S $L_{2,3}$ XES of thiophenes.

TABLE III. Observed peaks, emission energy, orbital nature, and functional group for C $K\alpha$ XES of P3HT.

Observed peaks (eV)	Emission energy[a] [CEBE-VIP] (eV)	Orbital nature	Functional group
wing[b]	268.4–274.0	s_{σ}(C2sC2p-C2s)-B	-C-C in hexyl chain
(265–272)[c]	265.4–268.1	s_{σ}(C2sC2p-C2s;S3s)-B	-C=C,-C-S in thiophene ring
274	274.4–276.1	p_{σ}(C2s-C2p;S3p)-B	-C=C,-C-S in thiophene ring
(272–275)[c]			
277	276.5–280.4	P_{σ}(C2p-C2p)-B	-C-C in hexyl chain
(275–279)[c]		p_{π}(C2p-C2p;S3p)-B	-C=C,-C-S in thiophene ring
280	281.5–284.1	p_{π}(C2p-C2p;S3p)-B	-C=C,-C-S in thiophene ring
(279–282)[c]	280.5–281.7	p_{σ}(C2p-C2p)-B	-C-C in hexyl chain

[a] The emission energy $[(\mathrm{CEBE})_{Is}-(\mathrm{VIP},I_k)]_{j[2p(A)]}$ is obtained from the difference between core-level binding energies(CEBE) and the vertical ionization potentials (VIP's) of the electrons that refill the core hole.

[b] ''Wing'' indicates that the decay line approaches the horizontal line.

[c] Peak range.

F 2p and C 2p states from C—F bonding form the peaks *E-D* of the UPS. The peaks *C*, *B*, and *A* (at 8–0 eV) of UPS arise from C 2p and N 2p components of C—N bonding and Cu 3d4s states of neighboring Cu atoms.

B. Thiophenes

The dominant influence of the local surrounding on the formation of x-ray emission spectra for the constituents is also found for thiophenes. C $K\alpha$ and S $L_{2,3}$ XES, which probe C 2p and S 3s3d occupied state densities, respectively, are found to be nearly identical for P3HT and DHα4T (Fig. 5). The thiophenlike motive is present in the chemical structure of both compounds (Fig. 2) and determines the fine structure of $K\alpha$ and S $L_{2,3}$ XES. It is especially interesting that the contribution of the side group R=$C_{16}H_{13}$ to the formation of C $K\alpha$ XES of P3HT is found to be negligible. This indicates that the electronic structure of the π system is not affected by the presence of the side group. This conclusion is in an agreement with results of optical absorption and photoemission measurements as well as theoretical calculations (see Ref. 25).

The fine structure of C $K\alpha$ XES of P3HT and DHα4T with its two rather broad subbands located at 276.8 and 280.0 eV is very similar to that of amorphous carbon (a-C) (see Fig. 5) with mainly sp^2 configuration. It indicates that

TABLE IV. Observed peaks, emission energy, orbital nature, and functional group for C $K\alpha$ XES of DHα4T.

Observed peaks (eV)	Emission energy[a] [CEBE-VIP] (eV)	Orbital nature	Functional group
Wing[b]	268.1–271.4	s_{σ}(C2sC2p-C2s;S3s)-B	-C=,-C-S in thiophene ring
(265–272)[c]	264.7–266.2		
274	272.6–276.6	p_{σ}(C2s-C2p;S3p)-B	-C=C,-C-S in thiophene ring
(272–275)[c]			
277	277.2–280.6	p_{σ}(C2p-C2p;S3p)-B	-C=C,-C-S in thiophene ring
(275–279)[c]			
280	281.3–283.7	p_{π}(C2p-C2p;S3p)-B	-C=C,-C-S in thiophene ring
(279–282)[c]			

[a] The emission energy $[(\mathrm{CEBE})_{Is}-(\mathrm{VIP},I_k)]_{j[2p(A)]}$ is obtained from the difference between core-level binding energies(CEBE) and the vertical ionization potentials (VIP's) of the electrons that refill the core hole.

[b] ''Wing'' indicates that the decay line approaches the horizontal line.

[c] Peak range.

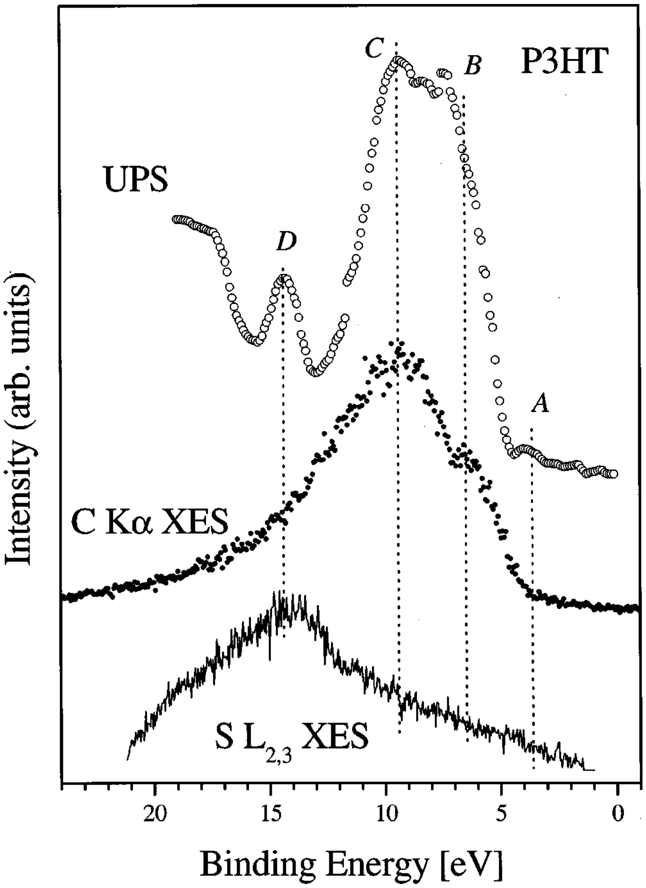

FIG. 6. Comparison of x-ray emission and UPS (Ref. 25) spectra of P3HT.

carbon atoms in thiophenes are present mainly in the sp^2-hybridized state. This is in agreement with estimations given in Ref. 25, based on an analysis of changes in the calculated charge changes. A chemical shift has been observed for C 1s XPS in different compounds. DeMon DFT calculations of PH3T support our interpretation of the C $K\alpha$ emission.

The calculated C $K\alpha$ and S $L_{2,3}$ XES of model molecules for PH3T and DHα4T are in good agreement with the experimental spectra (Fig. 5 and Tables III–IV). According to the DFT calculations, the main peaks located at 277 and 280 eV originate from p_σ(C2p-C2p) and p_π(C2p-C2pS3p) bonding orbitals of hexyl chains and thiophene groups. It is found that the C_6H_{13} side group does not contribute noticeably to the C $K\alpha$ emission of P3HT.

We have compared C $K\alpha$ and S $L_{2,3}$ XES (converted to the binding-energy scale) with UPS of P3HT [Ref. 25] in Fig. 6. The peak *D* at the highest binding energy in the photoemission spectrum (16–13 eV) arises from S 3s states because the intensity maximum of S$L_{2,3}$XES has the same binding energy. The next three peaks *C*, *B*, and *A* are formed mainly by C 2p and S 3p states. The intensity ratio of UPS peaks *B* to *C* is higher than that of C $K\alpha$ XES, showing that S 3p states contribute to peak *B*. S 3p states are not revealed in the S $L_{2,3}$ emission due to the dipole selection rule but can be seen in the S $K\beta_{1,3}$ emission ($3p \rightarrow 1s$ transitions). From the comparison of UPS and XES of P3HT we find reasonable agreement with recent band-structure calculations of bulk thiophenes (see Refs. 26–28). According to these calculations, a rather broad subband *A* of UPS and C $K\alpha$ XES of P3HT can be attributed to the delocalized character of the C 2p wave functions situated along the polymer.

IV. CONCLUSION

To conclude, x-ray emission spectra combined with photoemission measurements and theoretical deMon DFT calculations give a detailed description of the electronic structure of organic semiconductors. We have found that the electronic structure of such π systems as thipohenes is characterized by the delocalized character of C 2p wave functions along the polymer backbone and is not affected by the presence of the side group. The ratio of the emission intensities $\mathrm{CuL}_2/\mathrm{Cu}L_3$ is found to be two times less for CuPc and F_{16}CuPc than for Cu metal, which evidences strong covalency effects in phtalocyanines.

ACKNOWLEDGMENTS

This paper was supported by the Russian Foundation for Basic Research (Project Nos. 00-15-96575 and 99-03-32503), NATO Collaborative Linkage Grant, and the President's NSERC fund of the University of Saskatchewan. The work at the Advanced Light Source at Lawrence Berkeley National Laboratory was supported by the U.S. Department of Energy (Contract No. DE-AC03-76SF00098).

---

[1] F. Garnier, R. Hajlaoui, A. Yassar, and P. Srivastava, Science **265**, 1684 (1994).
[2] A. J. Lovinger and L. J. Rothberg, J. Mater. Res. **11**, 1581 (1996).
[3] G. Horowitz, Adv. Mater. **10**, 365 (1998).
[4] H. Koezuka, A. Tsumore, and T. Ando, Synth. Met. **18**, 699 (1987).
[5] A. Dadabalapur, H. E. Katz, L. Torsi, and R. C. Haddon, Science **269**, 1560 (1995).
[6] J. Kastner, J. Paloheimo, H. Kuzmany, in *Springer Series in Solid State Science* edited by H. Kuzmany, M. Mehring, and J. Fink (Springer-Verlag, Berlin, 1993), Vol. 113, pp. 512.
[7] R. C. Haddon, A. S. Perel, R. C. Morris, T. T. M. Palstra, A. F. Hebard, and R. M. Fleming, Appl. Phys. Lett. **67**, 121 (1995).
[8] Z. Bao, A. J. Lovinger, and J. Brown, J. Am. Chem. Soc. **120**, 207 (1998).
[9] A. St-Amant and D. R. Salahub, Chem. Phys. Lett. **169**, 387 (1990); A. St-Amant, Ph.D. thesis, University of Montreal, 1991.
[10] J. J. Jia, T. A. Callcott, J. Yurkas, A. W. Ellis, F. J. Himpsel, M. G. Samant, J. Stöhr, D. L. Ederer, J. A. Carlisle, E. A. Hudson, L. J. Terminello, D. K. Shuh, and R. C. C. Perera, Rev. Sci. Instrum. **66**, 1394 (1995).

[11] H. E. Katz, A. J. Lovinger, and J. G. Laquindanum, Chem. Mater. **10**, 457 (1998).

[12] M. J. S. Dewar and E. G. Zoebisch, THEOCHEM **180**, 1 (1988); M. J. S. Dewar, E. G. Zoebisch, E. F. Healy, and J. J. P. Stewart, J. Am. Chem. Soc. **107**, 3902 (1985).

[13] A. D. Becke, Phys. Rev. A **38**, 3098 (1988).

[14] J. P. Perdew, Phys. Rev. B **33**, 8822 (1986).

[15] P. Skytt, J.-H. Guo, N. Wassdahl, J. Nordgren, Y. Luo, and H. Agren, Phys. Rev. A **52**, 3572 (1995).

[16] E. Z. Kurmaev, V. R. Galakhov, A. Moewes, S. Shimada, K. Endo, S. S. Turner, P. Day, R. N. Lyubovskaya, D. L. Ederer, and M. Iwami, Phys. Rev. B **62**, 11 380 (2000).

[17] S. M. Butorin, V. R. Galakhov, E. Z. Kurmaev, and V. I. Glazyrina, Solid State Commun. **81**, 1003 (1992).

[18] J. E. Holliday, in *Band Structure Spectroscopy of Metals and Alloys*, edited by D. J. Fabian and L. M. Watson (Academic, London, 1973), pp. 713.

[19] H. W. Skinner, T. G. Bullen, and J. Jonston, Philos. Mag. **45**, 1070 (1954).

[20] V. R. Galakhov, E. Z. Kurmaev, and V. M. Cherkashenko, Izv. AN SSSR, Ser. Fiz. (USSR) **49**, 1513 (1985).

[21] V. R. Galakhov and E. Z. Kurmaev, Poverkhnost. Fizika, Khimiya, Mekhanika (USSR) **10**, 107 (1987).

[22] J. Kawai, S. Tsuboyama, K. Ishizu, K. Miyamura, and M. Saburi, Anal. Sci. **10**, 853 (1994).

[23] T. Chasse, C. I. Wu, I. G. Hill, and A. Kahn, J. Appl. Phys. **85**, 6589 (1999).

[24] T. Shimada, K. Hamaguchi, and A. Koma, Appl. Phys. Lett. **72**, 1869 (1998).

[25] R. Lazzaroni, M. Logdlund, S. Stafstrom, and W. R. Salaneck, J. Chem. Phys. **93**, 4433 (1990).

[26] J.-W. van der Horst, P. A. Bobbert, M. A. J. Michels, G. Brocks, and P. J. Kelly, Phys. Rev. Lett. **83**, 4413 (1999).

[27] J.-W. van der Horst, P. A. Bobbert, P. H. L. de Jong, M. A. J. Michels, G. Brocks, and P. J. Kelly, Phys. Rev. B **61**, 15 817 (2000).

[28] M. Shatzmayr, G. Koller, I. Kardinal, M. G. Ramsey, S. Stafstrom, and F. P. Netzer, J. Chem. Phys. **110**, 8060 (1999).

[29] F. Aryasetiawan and O. Gunnarsson, Rep. Prog. Phys. **61**, 237 (1998).

[30] V. I. Anisimov, F. Aryasetiawan, and A. I. Lichtenstein, J. Phys.: Condens. Matter **9**, 767 (1997).